Modal and Aeroelastic Analysis of A High-Aspect-Ratio Wing with Large Deflection Capability

R. Koohi*
Department of, Mechanical and Aerospace Engineering, Science and Research Branch, Islamic Azad University, Tehran, Iran
E-mail: koohi@iaukhsh.ac.ir
*Corresponding author

H. Shahverdi
Department of Aerospace Engineering and Center of Excellence in Computational Aerospace,
Amirkabir University of Technology, Tehran, Iran
E-mail: h_shahverdi@aut.ac.ir

H. Haddadpour
Department of Aerospace Engineering,
Sharif University of Technology, Tehran, Iran
E-mail: haddadpour@sharif.edu

Received: 19 August 2014, Revised: 22 October 2014, Accepted: 4 October 2014

Abstract: This paper describes a modified structural dynamics model for aeroelastic analysis of high-aspect-ratio wings undergoing large deformation behavior. To achieve this objective, a moderate deflection beam model is modified with some important large deflection terms and then coupled with a state space unsteady aerodynamics model. Finite element method is used to discretize the equations of motion. A dynamic perturbation equation about a nonlinear static equilibrium is applied to determine the flutter boundary. The obtained results show good agreement in comparison with other existing data such as high-altitude long-endurance (HALE) wing and Goland wing. It is found that the present aeroelastic tool have a good agreement in comparison with valid researches and also considering the effect of the geometric structural nonlinearity and higher order nonlinear terms on the flutter boundary determination is very significant.

Keywords: FEM, Jone's Approximate Unsteady Aerodynamics, Large Deflection, Wing Aeroelastic Stability

Reference: Koohi, R., Shahverdi, H., and Haddadpour, H., 'Modal and Aeroelastic Analysis of A High-Aspect-Ratio Wing with Large Deflection Capability', Int J of Advanced Design and Manufacturing Technology, Vol. 8/No. 1, 2015, pp. 45-54.

Biographical notes: R. Koohi received his PhD in Aerospace Engineering from IAU University, Science and Research Branch in 2014. He is currently Assistant Professor at the Mechanical Engineering Department, IAU, Khomeini Shahr, Iran. **H. Shahverdi** is Associate Professor of Aerospace engineering at the Amirkabir University of Technology, Iran. He received his PhD in Aerospace engineering from Amirkabir University of Technology in 2006. **H. Haddadpour** is Professor of Aerospace engineering at the Sharif University of Technology, Iran. He received his PhD in mechanical engineering from University of Tehran in 2002.

1 INTRODUCTION

In the study of wing aeroelastic problems, linear models are usually implemented, while these models have some restrictions such as small deflections and low angle of attack. However considering moderate or large deflections causes structural geometric nonlinearity and performing nonlinear analysis is so necessary. In a high aspect ratio wing, flexibility factor coupled with the long span results in the possibility of large deflections during normal flight condition and so the stiffness and natural frequencies of the wing may be changed. Hence in aeroelastic analysis of the high aspect ratio wings, nonlinear models must be implemented for predicting the instability limits.

There is too much attention paid to nonlinear aeroelastic analysis in the last two decades. Many researchers investigated the effects of aerodynamic stall nonlinearity, structural geometry nonlinearity and free play nonlinearity on the aeroelastic behavior of typical section model as well as cantilevered wing model. In nonlinear aeroelastic analysis, the system can be simulated in time domain or in frequency domain. In the time domain method, the system is marched in time for various initial conditions and the response is gained in the form of time-varying curves or phase planes. If the speed reaches a critical value, instability occurs. In this case, the trajectories tend towards a limit cycle oscillations (LCO). In the frequency domain method, the dynamic perturbation equations are linearized about a nonlinear static equilibrium conditions to determine the stability boundaries.

In order to construct models of nonlinear aeroelastic systems properly, appropriate nonlinear models and solution methods are required. Hodges and Dowell provided nonlinear equations with quadratic nonlinearities for rotor blades undergoing large deformations [1]. Dowell et al., compared their experimental results with the Hodges-Dowell equations, and showed that there are some differences between analytical and experimental results [2]. These differences are due to elimination of higher order nonlinear terms in the Hodges-Dowell model. Hodges et al., showed that the bending deflection equations should also involve third order nonlinear terms [3]. Rosen and Friedmann presented more accurate system of equations than those of Hodges-Dowell because they considered additional higher order nonlinear terms, so their results were in better agreement with experimental results obtained by Dowell et al., [2], [4].

Crespo da Silva and Glynn applied the extended form of Hamilton's principle to develop a set of mathematically consistent nonlinear equations [5]. Cubic terms were not shown explicitly in their equations but these equations fully included the contributions due to nonlinear curvature and nonlinear inertia. Using these equations, nonlinear analysis of a cantilever beam was performed [6]. Also, these equations were developed to the case of composite beams by Pai and Nayfeh [7]. Hodges presented a general beam theory based on a nonlinear intrinsic formulation for the dynamics of initially curved and twisted beams in a moving frame [8]. This beam model is valid for both isotropic and composite materials.

In order to investigate the aeroelastic stability of a nonlinear beam, it is essential that its structural dynamics equations are combined with a suitable aerodynamic model. Tang and Dowell studied the aeroelastic response of a high-aspect ratio wing [9], [10]. The presented equations by Hodges-Dowell were used for modeling the structural nonlinearity and the semi-experimental aerodynamics (ONERA stall model) was used to describe the nonlinear aerodynamics [1]. Patil and Hodges investigated nonlinear aeroelastic behavior of a complete aircraft with high aspect-ratio wings based on geometrically-exact nonlinear equations for the beam structural dynamics and the finite-state aerodynamic theory of Peters along with the ONERA dynamic stall model [8], [11-13].

Yuan and Friedmann performed nonlinear aeroelastic analysis of a composite rotor blade using finite element method and quasi-steady aerodynamic theory [14], [15]. In this composite blade model, higher order terms associated with the strain–displacement relations are neglected using an ordering scheme, which appropriates for moderate deflection (small strain and moderate rotations) analysis. The moderate deflection simplification is justified for composite helicopter rotor blade analysis since rotor blades are designed from low stress and long-cycle fatigue considerations [16]. Friedmann et al., combined their previous work with an improved finite element cross-sectional analysis code (VABS) that was based on Hodges equations for application of composite materials [14], [16]. VABS also has been used to calculate the cross-sectional properties needed as inputs for other rotorcraft analysis codes [17], [18], [19].

Friedmann et al., [16] model accounts for arbitrary cross-sectional warping, in-plane stresses, and moderate deflections. In moderate deflection ordering schemes that also used by Hodges and Dowell, a second order approximation implies that terms of order ε^2 are neglected compared to terms of order 1, where ε is blade bending slope [1]. Some studies also used a third order approximation where terms of order ε^3 were neglected compared to terms of order 1 [5], [6]. The importance of using higher order terms in large deflections also noted in other studies [20-22]. Hodges developed a nonlinear beam kinematics in which the assumption of moderate rotation was removed [23]. This model was subsequently employed as the

theoretical basis for the beam element used in the computer program GRASP. Also some other researchers investigated vibration analysis of thin plates or beams [24-26].

In this study, Finite Element Method (FEM) is implemented for nonlinear aeroelastic analysis of a wing considering large deflections during normal flight condition that are not used by previous mentioned references. Therefore a nonlinear beam element is used to model wing's structural dynamics behaviour. An unsteady nonlinear aerodynamic theory is used for aerodynamic loading computation. Structural modeling is based on the presented model by Yuan and Friedmann [14]. But, the Yuan-Friedmann equations are developed for helicopter rotor blade application, moderate deflection and quasi-steady aerodynamic. However, in this study these equations have been modified for the case of fixed wings and to overcome previous model's large deformation modelling weakness, some important higher order terms are considered in this study. Also, the unsteady aerodynamic states model based on Jones's approximation is implemented for constructing an appropriate aeroelastic tool. Finally, the aeroelastic analyses for a certain test case are performed and the obtained results are compared and validated with those available in the literature.

2 STRUCTURAL DYNAMICS SIMULATION

To simulate the structural dynamic behavior of a wing, it can be discretized by utilizing several beam type elements along its elastic axis. The cross-section of the wing has a general shape with distinct shear center, tension center and center of mass. Angle of attack and pre-twist are included in this model. The nonlinear strain–displacement relations are developed from a moderate deflection theory (small strains and moderate rotations) with some important large deflection terms. Nonlinear equations of motion for each beam element are derived based on Hamilton's principle.

2.1. Coordinate systems

Several coordinate systems are required to describe deformation of the wing as shown in Figs. 1 and 2. The first two systems, $\left(\hat{e}_x,\hat{e}_y,\hat{e}_z\right)$ and $\left(\hat{e}_x,\hat{e}_\eta,\hat{e}_\zeta\right)$, respectively, are used to determine the position and orientation of each beam element relative to the wing root in the unreformed configuration. The vector $\hat{e}_x$ is aligned with the beam element elastic axis and the vectors $\hat{e}_y$ and $\hat{e}_z$ are defined in the cross-section of the beam. Wing pre-twist angle and angle of attack have been taken into account by θ_0 as shown in Fig. 1. This angle is defined as the change in the orientation of $\hat{e}_\eta,\hat{e}_\zeta$ with respect to $\hat{e}_y,\hat{e}_z$. The vectors $\hat{e}_\eta$ and $\hat{e}_\zeta$ are assigned parallel to the modulus weighted principal axes of the cross-section. The beam element strain–displacement relations are derived in $\left(\hat{e}_x,\hat{e}_\eta,\hat{e}_\zeta\right)$ system. However, $\left(\hat{e}'_x,\hat{e}'_\eta,\hat{e}'_\zeta\right)$ coordinate system is used to state the orientation of the local wing geometry after deformation. The orientation of $\left(\hat{e}'_x,\hat{e}'_\eta,\hat{e}'_\zeta\right)$ is obtained by rotating $\left(\hat{e}_x,\hat{e}_\eta,\hat{e}_\zeta\right)$ coordinate system through three Euler angles in the order of $\theta_\zeta,\theta_\eta,\theta_x$ about $\hat{e}_\zeta$ rotated $\hat{e}_\eta$ and rotated $\hat{e}_x$, respectively. This sequence was chosen to follow the work of previous authors.

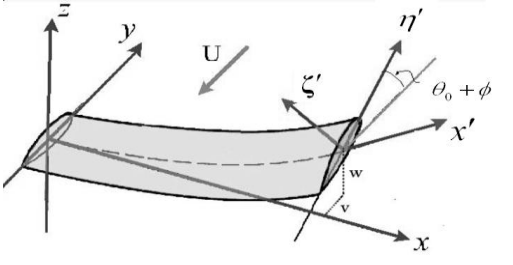

Fig. 1 Wing coordinate systems and deflections

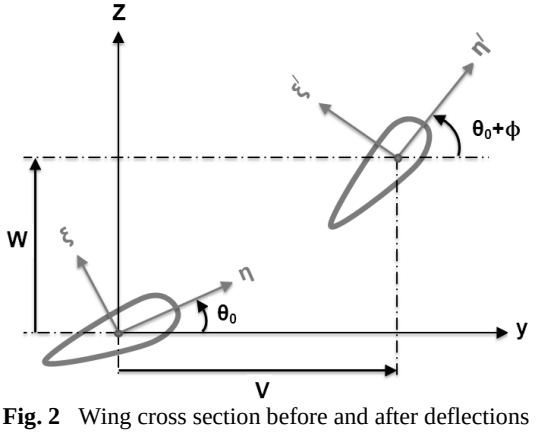

Fig. 2 Wing cross section before and after deflections

2.2. Constitutive relations

The constitutive relations are defined based on the assumptions of the linear elastic orthotropic model and the zero stress components within the cross-section $\left(\sigma_{\eta\eta}=\sigma_{\zeta\zeta}=\sigma_{\eta\zeta}=0\right)$. Using these assumptions the constitutive relations are:

$$\begin{bmatrix}\sigma_{xx}\\ \sigma_{x\zeta}\\ \sigma_{x\eta}\end{bmatrix}=\begin{bmatrix}Q_{11} & Q_{15} & Q_{16}\\ Q_{15} & Q_{55} & Q_{56}\\ Q_{16} & Q_{56} & Q_{66}\end{bmatrix}\begin{bmatrix}\varepsilon_{xx}\\ \gamma_{x\zeta}\\ \gamma_{x\eta}\end{bmatrix} \quad (1)$$

2.3. Aerodynamic modeling

For a two-dimensional airfoil undergoing sinusoidal motion in pulsating incompressible flow, based on Greenberg's extension of Theodorsen's theory and using Jone's approximation unsteady aerodynamics theory, the unsteady aerodynamic lift (L) and pitching moment (M) per unit span about the elastic axis can be expressed [27], [28].

$$\begin{aligned}L &= 0.5\,a\rho_A b^2\left[-\dot{U}_{\zeta'} - x_A - 0.5b\ \ddot{\theta}\right]\\ &\quad + a\rho_A b\ U_{\eta'} - U_{\zeta'}\theta\left[0.5\ -U_{\zeta'} + b - x_A\ \dot{\theta}\ -\sum_{i=1}^{n}\gamma_i B_i\right]\\ M &= -0.5\,a\rho_A b^2\{\ x_A - 0.5b\ \dot{U}_{\zeta'} + 0.5b\ U_{\eta'} - U_{\zeta'}\theta\ \dot{\theta}\\ &\quad + \left[(1/8)b^2 + x_A - 0.5b\ \ddot{\theta}\right]\}\\ &\quad + a\rho_A b x_A\ U_{\eta'} - U_{\zeta'}\theta\left[0.5(-U_{\zeta'} + (b - x_A)\dot{\theta}) - \sum_{i=1}^{n}\gamma_i B_i\right]\end{aligned} \quad (2)$$

Also, the profile drag per unit span is defined as:

$$D = C_{d0}\rho_A b(U_{\eta'}{}^2 + U_{\zeta'}{}^2) \quad (3)$$

Where a is the lift curve slope of the wing section; b is the semi-chord; ρ_A is air density; θ is the pitch angle with respect to free-stream and x_A is the non-dimensional distance between the aerodynamic center and the elastic axis of the airfoil cross-section, positive for aerodynamic center ahead of the elastic axis. The velocity vector of a point on the elastic axis of the wing relative to the air is:

$$\mathbf{U} = \mathbf{V_{EA}} - \mathbf{V_A} = U_x\hat{e}_{x'} + U_\eta\hat{e}_{\eta'} + U_\zeta\hat{e}_{\zeta'} \quad (4)$$

$$\begin{Bmatrix}V_x^{EA}\\ V_y^{EA}\\ V_z^{EA}\end{Bmatrix}=\begin{Bmatrix}0\\ \dot{v}\\ \dot{w}\end{Bmatrix},\quad \begin{Bmatrix}V_x^{A}\\ V_y^{A}\\ V_z^{A}\end{Bmatrix}=\begin{Bmatrix}0\\ -V_F\\ 0\end{Bmatrix}$$

And

$$\begin{Bmatrix}U_{x'}\\ U_{\eta'}\\ U_{\zeta'}\end{Bmatrix}=\left[\mathbf{T_{de}}\right]\begin{Bmatrix}V_x^{EA} - V_x^{A}\\ V_y^{EA} - V_y^{A}\\ V_z^{EA} - V_z^{A}\end{Bmatrix} \quad (5)$$

Where V_F is the free-stream velocity and the transformation matrix $\left[\mathbf{T_{de}}\right]$ that will be explained later. Also, B_i is the aerodynamic state according to Jone's approximate unsteady aerodynamics theory [28] which satisfies:

$$\dot{B}_i + (\beta_i V_F / b)B_i = U_{\zeta'} - b - x_A\ \dot{\theta} \quad (6)$$

Where

$$\gamma_i = V_F\beta_i\alpha_i / b.$$

The constants $\alpha_{i,}$ and β_i are the coefficients used in the quasi-polynomial approximation of the Wagner function that for the first and second states are:

$$\alpha_1 = 0.165;\quad \alpha_2 = 0.335;\quad \beta_1 = 0.0455;\quad \beta_2 = 0.3$$

2.4. Structural formulation

In this study, the nonlinear kinematics of deformation is based on the mechanics of curved rods [14]. The kinematical assumptions used in [14] are: (1) the deformations of the cross-section in its own plane are neglected; (2) the strain components are small compared to unity. But in the present study, besides the mentioned assumptions, the axial shear strains and warping terms are also neglected. The strain components after applying the ordering scheme become:

$$\begin{aligned}\varepsilon_{xx} &= u_{,x} + \frac{1}{2}(v_{,x})^2 + \frac{1}{2}(w_{,x})^2 - v_{,xx}\left[\eta\cos(\theta_0+\phi) - \zeta\sin(\theta_0+\phi)\right]\\ &\quad - w_{,xx}\left[\eta\sin(\theta_0+\phi) + \zeta\cos(\theta_0+\phi)\right] + \frac{1}{2}\left(\eta^2+\zeta^2\right)\left(\phi_{,x}\right)^2\\ \gamma_{x\eta} &= -\zeta\left(\phi_{,x} + \phi_0\right)\\ \gamma_{x\zeta} &= \eta\left(\phi_{,x} + \phi_0\right)\end{aligned} \quad (7)$$

Where, v, w, ϕ are out of plane and inplane deflection and twist at the elastic axis, respectively (Figs. 1 and 2). Using Hamilton's principle for each beam element, one can derive the non-linear equations of motion and the corresponding finite element matrices:

$$\int_{t1}^{t2}\left(\delta U - \delta T - \delta W\right)_e dt = 0 \quad (8)$$

Where δU, δT and δW_e are the variation of strain energy, kinetic energy, and virtual work of external loads, respectively.

2.4.1. Strain energy

The variational form of strain energy is

$$\delta U = \int_0^{l_e}\iint_A \begin{Bmatrix}\delta\varepsilon_{xx}\\ \delta\gamma_{x\zeta}\\ \delta\gamma_{x\eta}\end{Bmatrix}^T \begin{bmatrix}Q_{11} & Q_{15} & Q_{16}\\ Q_{15} & Q_{55} & Q_{56}\\ Q_{16} & Q_{56} & Q_{66}\end{bmatrix}\begin{bmatrix}\varepsilon_{xx}\\ \gamma_{x\zeta}\\ \gamma_{x\eta}\end{bmatrix} d\eta\, d\zeta\, dx. \quad (9)$$

The small angle assumption for ϕ yields:

$$\begin{aligned}&\cos(\theta_0+\phi)=\cos(\theta_0)-\phi\sin(\theta_0);\\ &\sin(\theta_0+\phi)=\sin(\theta_0)+\phi\cos(\theta_0)\end{aligned} \quad (10)$$

Thus, the variation of the left hand side of Eq. (10) is:

$$\begin{aligned}&\delta\cos(\theta_0+\phi)=-(\delta\phi)\sin(\theta_0+\phi)=-(\delta\phi)(\sin(\theta_0)+\phi\cos(\theta_0))\\ &\delta\sin(\theta_0+\phi)=(\delta\phi)\cos(\theta_0+\phi)=(\delta\phi)(\cos(\theta_0)-\phi\sin(\theta_0))\end{aligned} \quad (11)$$

However, the variation of the right hand side of Eq. (10) is

$$\begin{aligned}&\delta(\cos(\theta_0)-\phi\sin(\theta_0))=-\delta\phi\sin(\theta_0);\\ &\delta(\sin(\theta_0)+\phi\cos(\theta_0))=\delta\phi\cos(\theta_0)\end{aligned} \quad (12)$$

The main deference between the present study and Ref. [14], is that, in the present study, Eq. (10) is implemented after taking variation of axial strain, ε_{xx}, that results in Eq. (11) and keeps higher order terms, which is important in large deflection computations but in Ref. [14] these terms did not appear because Eq. (10) has been used before taking variation of ε_{xx} that yields to Eq. (12). Integrating Eq. (9) over the cross-section gives modulus weighted section constants, which are presented in Ref. [14]. These section constants can be calculated using separate, one-dimensional linear beam analysis.

2.4.2. Kinetic energy

The variation of the kinetic energy for each beam element is:

$$\delta T = \int_0^{l_e}\iint_A \rho\mathbf{V}.\delta\mathbf{V}\, d\eta\, d\zeta\, dx \quad (13)$$

Where the velocity vector, $\mathbf{V}$, is obtained by

$$\mathbf{V}=\dot{\mathbf{R}} \quad (14)$$

The position vector, $\mathbf{R}$, of a point on the deformed beam is written in the following form

$$\mathbf{R}=(h_e+x)\hat{e}_x+v\hat{e}_y+w\hat{e}_z+\eta\hat{e}'_\eta+\zeta\hat{e}'_\zeta \quad (15)$$

All the terms in the velocity vector were transformed to the $(\hat{e}_x,\hat{e}_y,\hat{e}_z)$ coordinate system by:

$$\begin{Bmatrix}\hat{e}'_x\\ \hat{e}'_\eta\\ \hat{e}'_\zeta\end{Bmatrix}=[\mathbf{T_{de}}]\begin{Bmatrix}\hat{e}_x\\ \hat{e}_y\\ \hat{e}_z\end{Bmatrix} \quad (16)$$

Where the transformation matrix $[\mathbf{T_{de}}]$ is expressed as:

$$[\mathbf{T_{de}}]=\begin{bmatrix}1 & v_{,x} & w_{,x}\\ -v_{,x}\cos(\theta_0+\phi)-w_{,x}\sin(\theta_0+\phi) & \cos(\theta_0+\phi) & \sin(\theta_0+\phi)\\ v_{,x}\sin(\theta_0+\phi)-w_{,x}\cos(\theta_0+\phi) & -\sin(\theta_0+\phi)+\tau'_c\cos(\theta_0) & \cos(\theta_0+\phi)+\tau'_c\sin(\theta_0)\end{bmatrix} \quad (17)$$

Where

$$\tau'_c=(v_{,x}\sin\theta_0-w_{,x}\cos\theta_0)(v_{,x}\cos\theta_0+w_{,x}\sin\theta_0) \quad (18)$$

Integrating Eq. (13) over the cross-section yields mass weighted section constants about the shear center.

2.4.3. External work contributions

Using the principle of virtual work, the effects of the non-conservative distributed loads are involved. The virtual work on each beam element is defined as:

$$\delta W_e = \int_0^{le}(\mathbf{P}.\delta\mathbf{u}+\mathbf{Q}.\delta\vec{\boldsymbol{\theta}})dx \quad (19)$$

Where, P and Q are the distributed aerodynamic force and moment vectors along the elastic axis; $\delta\mathbf{u}$ and $\delta\vec{\boldsymbol{\theta}}$ are the virtual displacement and rotation vectors, respectively, of a point on the deformed elastic axis.

3 SOLUTION METHODOLOGY

In this study, the finite element method is implemented for solving the system of aeroelastic equations. Therefore, the wing is divided into several beam elements. The discretized form of Hamilton's principle is written as

$$\int_{t1}^{t2}\sum_{i=1}^{n}(\delta U_i-\delta T_i-\delta W_{ei})dt=0 \quad (20)$$

Where n is the total number of beam elements. The Hermitian shape functions are used to discretize the

space dependence: cubic polynomials for v and w ; quadratic polynomials for ϕ .

$$v = \{\mathbf{\Phi_c}\}^T \{\mathbf{V}\}, \quad w = \{\mathbf{\Phi_c}\}^T \{\mathbf{W}\}, \quad \phi = \{\mathbf{\Phi_q}\}^T \{\mathbf{\Phi}\} \tag{21}$$

Each beam element consists of two end nodes and one internal node at its mid-point, which results in 11 nodal degrees of freedom, as shown in Fig. 3. Thus,

$$\{\mathbf{V}\} = \begin{bmatrix} V_1 & V_{1,x} & V_2 & V_{2,x} \end{bmatrix}^T, \quad \{\mathbf{W}\} = \begin{bmatrix} W_1 & W_{1,x} & W_2 & W_{2,x} \end{bmatrix}^T, \quad \{\mathbf{\Phi}\} = \begin{bmatrix} \phi_1 & \phi_2 & \phi_3 \end{bmatrix}^T \tag{22}$$

The vector of element nodal degrees of freedom, $\mathbf{q}$, is defined as:

$$\mathbf{q} = \begin{bmatrix} \{\mathbf{V}\}^T & \{\mathbf{W}\}^T & \{\mathbf{\Phi}\}^T \end{bmatrix}^T \tag{23}$$

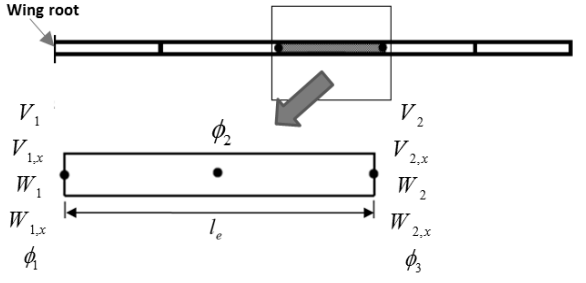

Fig. 3 Wing finite element model and related nodal degrees of freedom

Since the variation of the generalized coordinates $(\delta v, \delta w, \delta\phi)$ are arbitrary over the time interval, therefore $\delta\mathbf{q}$ is also arbitrary; and this results in the finite element equations of motion for the i[th] beam element, which is written as

$$[M_i]\{\ddot{q}\} + [K_i]\{q\} + \{F_i\} = 0 \tag{24}$$

Where $[M]$ is the structural mass matrix, $[K]$ is the stiffness matrix including linear structural stiffness matrix, nonlinear structural stiffness matrix and the nonlinear aerodynamic stiffness matrix that also is a function of the aerodynamic states. Also, the applied aerodynamic force vector, $\{F\}$ is a nonlinear function of deflections and theirs derivatives with respect to time. So, it includes the aerodynamic damping terms. After computing and assembling the mass, stiffness matrices and force vector, the natural frequencies and related mode shapes of the wing are firstly calculated.

Hence, for the free vibration analysis, the equations of motion for total elements are:

$$[M]\ddot{q} + [K^S]q = 0 \tag{25}$$

The superscript S denotes the linear structural matrix used in the free vibration analysis. After imposing the boundary conditions, a standard eigenvalue procedure is implemented to find the natural frequencies and mode shapes of the wing. In order to reduce the computational size of the problem, a modal coordinate transformation is then applied. For the i[th] element, the modal coordinate transformation has the following form:

$$q_i = [Q_i]y \tag{26}$$

The new unknowns of the problem, $\mathbf{y}$, is the vector of the generalized modal coordinates and has a size of N_m where N_m is the number of modes used to perform the modal coordinate transformation. The columns of $[Q_i]$ correspond to the portions of the normal mode eigenvectors for the i[th] element. The assembled matrices and load vector of the wing are obtained as follows:

$$[K] = \sum_{i=1}^{n} [Q_i]^T [K_i] [Q_i];$$

$$[C] = \sum_{i=1}^{n} [Q_i]^T [C_i] [Q_i];$$

$$[M] = \sum_{i=1}^{n} [Q_i]^T [M_i] [Q_i]; \quad [F] = \sum_{i=1}^{n} [Q_i]^T [F_i]; \tag{27}$$

After applying this transformation to Eq. (24) and introducing the aerodynamic states, a set of nonlinear, coupled, ordinary differential equations containing multiple variables is obtained as follows:

$$\mathbf{f} = \begin{bmatrix} \mathbf{M}_{eq} \end{bmatrix} \{\ddot{\mathbf{X}}\} + \begin{bmatrix} \mathbf{K}_{eq} \end{bmatrix} \{\mathbf{X}\} + \{\mathbf{F}_{eq}\} = \mathbf{0} \tag{28}$$

Where

$$\begin{bmatrix} M_{eq} \end{bmatrix} = \begin{bmatrix} M(y) & 0 \\ 0 & 0 \end{bmatrix},$$

$$\begin{bmatrix} K_{eq} \end{bmatrix} = \begin{bmatrix} K(y, \dot{y}, \ddot{y}, B, \dot{B}) & 0 \\ 0 & 0 \end{bmatrix},$$

$$\{F_{eq}\} = \begin{Bmatrix} F(y, \dot{y}, \ddot{y}, B, \dot{B}) \\ F_B(y, \dot{y}, B, \dot{B}) \end{Bmatrix} \tag{29}$$

The new unknowns generalized modal coordinate vector is:

$$\{X\} = \begin{Bmatrix} y \\ B \end{Bmatrix} \tag{30}$$

Here, $\{B\}$ is the Jones approximate unsteady aerodynamic states that has a size of $2n$ and is defined as:

$$\{B\} = \left\{B_1^1 B_2^1 B_1^2 B_2^2 \ldots B_1^n B_2^n\right\}^T \tag{31}$$

$\{F_B\}$ is the additional force vector for modeling the unsteady aerodynamic (Eq. (7)). The solutions of Eq. (28) can be expressed in the form:

$$X = X_0 + \Delta X \tag{32}$$

Where X_0 denotes steady-state solution and ΔX denotes the small perturbation on it. The static equilibrium position, X_0, is obtained from Eq. (28) by setting $\dot{X} = \ddot{X} = 0$ and solving the resulting nonlinear algebraic equations using iteratively by the Newton-Raphson method. Subsequently, Eq. (28) can be linearized about the nonlinear static equilibrium position X_0, to yield:

$$[\bar{M}(X_0)]\Delta\ddot{X} + [\bar{C}(X_0)]\Delta\dot{X} + [\bar{K}(X_0)]\Delta X + H.O.T = 0 \tag{33}$$

Where

$$[\bar{\mathbf{M}}] = \left[\partial \mathbf{f} / \partial \ddot{\mathbf{X}}\right]_{\mathbf{X}_0,\mathbf{0},\mathbf{0}} \quad [\bar{\mathbf{C}}] = \left[\partial \mathbf{f} / \partial \dot{\mathbf{X}}\right]_{\mathbf{X}_0,\mathbf{0},\mathbf{0}} \qquad [\bar{\mathbf{K}}] = \left[\partial \mathbf{f} / \partial \mathbf{X}\right]_{\mathbf{X}_0,\mathbf{0},\mathbf{0}} \tag{34}$$

Eq. (33), can be expressed in the first order state variable form after neglecting the higher order terms by:

$$\dot{z} = [A]z \tag{35}$$

Where the state vector $\mathbf{z}$ is defined as:

$$z = \begin{Bmatrix} \Delta X \\ \Delta \dot{X} \end{Bmatrix} \tag{36}$$

And the system matrix $\mathbf{A}$ has the following form:

$$A = \begin{bmatrix} [0] & [I] \\ -[\bar{M}]^{-1}[\bar{K}] & -[\bar{M}]^{-1}[\bar{C}] \end{bmatrix} \tag{37}$$

The stability of the system is investigated through the eigenvalue analysis of $\mathbf{A}$. Of course, these eigenvalues are complex conjugate pairs:

$$\lambda_j = \zeta_j \pm i\,\omega_j, \qquad j = 1,\ldots,N_m \tag{38}$$

The wing is stable if $(\zeta_i < 0)$ for all j.

4 RESULTS AND DISCUSSION

Two test cases including HALE wing and Goland wing are considered here to validate the present aeroelastic model. The relative characteristics are shown in Tables 1 and 2. For numerical simulation, the wing is discritized using 8 spanwise beam elements and the first 20 structural eigenmodes retained in the aeroelastic analysis $(n_m = 20)$.

Table 1 Input data for HALE wing [11]

Specification	Value
Half span (m)	16
Chord (m)	1m
Mass per unit length (kg/m)	0.75
Moment of Inertia (50% chord) (kg. m)	0.1
Spanwise elastic axis	50% chord
Center of gravity	50% chord
Bending rigidity (N m^2)	2×10^4
Torsional rigidity (N m^2)	1×10^4
Bending rigidity (edgewise) (N m^2)	4×10^6
Density of air kg/m^3	0.0889

Table 2 Input data for Goland wing [13]

Specification	Value
Half span (ft)	20
Wing chord (ft)	6
Mass per unit length (slugs/ft)	0.746
Radius of gyration about mass center	25% chord
Spanwise elastic axis (from l.e.)	33% chord
Center of gravity (from l.e.)	43% chord
Bending rigidity (lb ft^2)	23.65×10^6
Torsional rigidity (lb ft^2)	2.39×10^6
Air density (slugs/ ft^3)	0.002378

4.1. Linear Results

In this section the linear aeroelastic behavior of the present model is validated. Table 3 presents the computed HALE wing's natural frequencies with

neglecting all nonlinear effects. They are compared against the reported results in Refs. [11], [29]. The obtained results show very good agreement in comparison with the exact solution. Table 4 presents the obtained results from a linear aeroelastic analysis including flutter speed, flutter frequency and divergence speed of the pervious wing model.

Table 3 Comparison of the linear modal frequencies (rad/s) for Hale wing

	Present Analysis		Ref. [11]		Exact Solution [29]
	Value	Percentage error	Value	Percentage error	
1st Flat. Bend.	2.243	0.0	2.247	0.2	2.243
2nd Flat. Bend.	14.057	0.01	14.606	3.9	14.056
3rd Flat. Bend.	39.380	0.06	44.012	11.8	39.356
1st Torsion	31.046	0.0	31.146	0.3	31.046
1st Edge. Bend.	31.718	0.0	31.739	0.1	31.718

Table 4 Comparison of linear aeroelastic results for Hale wing

	Present Analysis		Ref. [12]		Ref. [29]
	Value	Error with [29]	Value	Error with [29]	
Flut. Speed (m/s)	32.67	%0.5	32.21	%0.9	32.51
Flut. Freq (rad/s)	22.07	%1.3	22.61	%1.1	22.37
Div. Speed (m/s)	37.19	%0.1	37.29	%0.4	37.15

Table 5 Comparison of linear aeroelastic results for Goland wing

	Present Analysis		Ref. [13]		Ref. [29]
	Value	Error with [29]	Value	Error with [29]	
Flutter Speed (ft/sec)	451	%0.2	445	%1.1	450
Flutter Freq(rad/s)	69.3	%2	70.2	%0.7	70.7

These are also compared with the presented results in Refs. [12], [29]. It must be noted that the presented results in Ref. [29] were obtained by the Rayleigh-Ritz structural analysis with uncoupled beam mode shapes and implementation of Theodorsen's strip theory for unsteady aerodynamics. These results are almost identical. Table 5 presents the obtained results for a linear calculation of flutter speed and frequency of Goland wing that show good agreement with those exist in Refs. [13], [29].

4.2. Nonlinear Results

To construct the eigenvalue problem of the considered nonlinear aeroelastic model, a concentrated force is added to the tip of Hale wing which causes deformation of the wing. Thus, the aeroelastic system can be expressed in the perturbation form about this deformation state (usual linearization method). The favorite results including, natural frequencies, flutter speed and frequency of aeroelastic model obtained by the solution of the perturbed eigenvalue problem. Figs. 4-6, respectively, show the first five structural natural frequencies, nonlinear flutter speed and frequency versus the tip static displacement for two cases of structural equations.

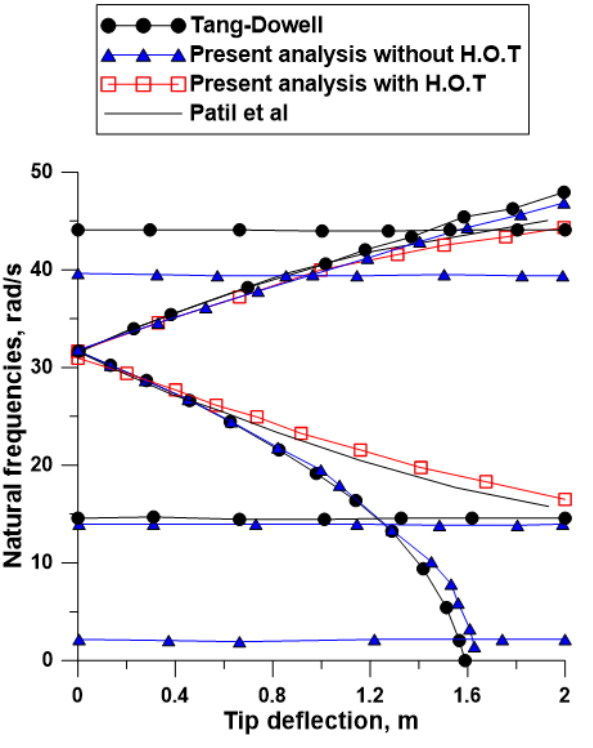

Fig. 4 Structural natural frequencies versus tip displacement

In the first case, Yuan and Friedmann equations are used and the associated results are simulated by the present method without higher order terms (H.O.T) [14]. In the second case only higher order terms, discussed in section 2.8, are considered in the first case and assigned as the present method with H.O.T. In order to make comparison, the reported results by Patil et al., and Tang and Dowell are also presented in Fig.

1[10], [11]. It must be noted that Tang and Dowell used Hodges-Dowell equations that did not include higher order terms and so their results are similar to the present method without H.O.T [10], [1]. Results of the present method with H.O.T are similar to those in Ref. [11] that used the geometrically exact formulation. The significant differences are seen in the range of the large tip displacements between both cases of with and without H.O.T in the present study. As it was shown here, the incorporating quadratic and cubic nonlinear terms due to large deflections behavior in aeroelastic analysis plays important role.

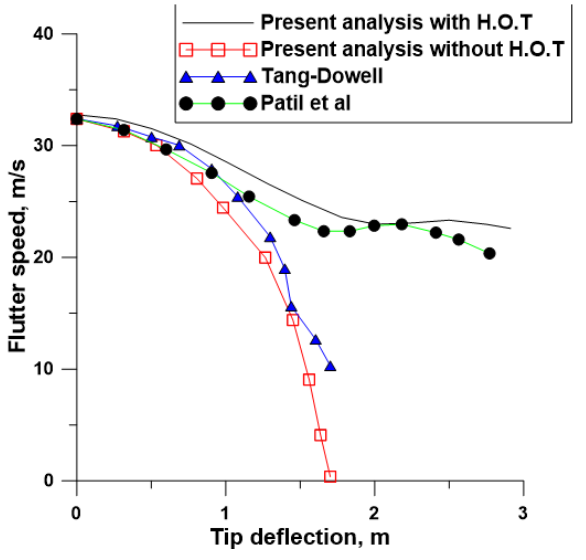

Fig. 5 Variation of flutter speed with tip displacement

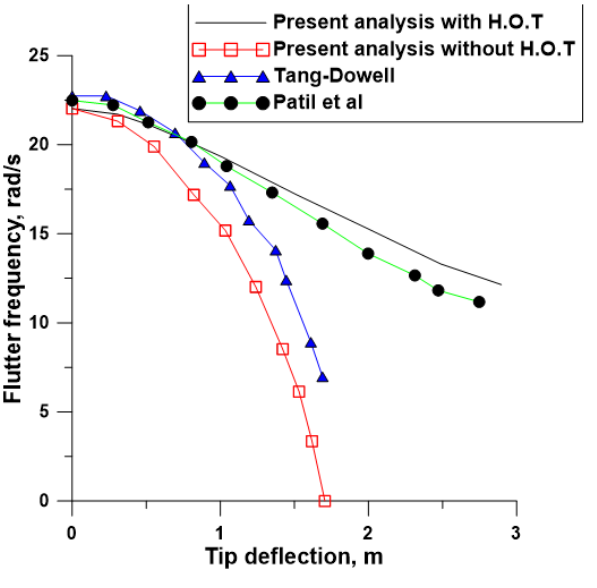

Fig. 6 Variation of flutter frequency with tip displacement

5 CONCLUDING REMARKS

A modified model with the capability of calculating the stability of wing was developed based on Hamilton's principle and using a finite element formulation. Numerical results including the natural frequencies and aeroelastic stability of the selected wing configurations, which show the effects of wing tip displacement, were presented and compared with those available in the literature. The following conclusions are also obtained:

- Incorporating Jones approximate unsteady aerodynamic model with the present structural model leads to an alternative applicable aeroelastic model for fixed wing analysis.
- It is essential to consider some higher order terms in structural equations of motion for large deflection problems.

REFERENCES

[1] Hodges, D. H., Dowell, E., "Nonlinear Equations of Motion for the Elastic Bending and Torsion of Twisted Non uniform Rotor Blades", NASA TN D-7818, 1974.

[2] Dowell, E., Traybar, J., and Hodges, D. H., "An Experimental-Theoretical Correlation Study of Nonlinear Bending and Torsion Deformations of a Cantilever beam", Journal of Sound and Vibration, Vol. 50, 1977, pp. 533-544.

[3] Hodges, D. H., Crespo da Silva, M., and Peters, D., "Nonlinear Effects in the Static and Dynamic Behavior of Beams and Rotor Blades", Vertica, Vol. 12, No. 3, 1988, pp. 243-256.

[4] Rosen, A., Freidmann, P. P., "The Nonlinear Behavior of Elastic Slender Straight Beams Undergoing Small Strains and Moderate Rotations", Journal of Applied Mechanics, Vol. 46, 1979, pp. 161-168.

[5] Crespo da Silva, M., Glynn, C., "Nonlinear Flexural-Flexural-Torsional Dynamics of Inextensional Beams-I. Equations of Motions", Journal of Structural Mechanics, Vol. 6, No. 4, 1978, pp. 437-448.

[6] Crespo da Silva, M., Glynn, C., "Nonlinear Flexural-Flexural-Torsional Dynamics of Inextensional Beams-I. Forced Motions", Journal of Structural Mechanics, Vol. 6, No. 4, 1978, pp. 449-461.

[7] Pai, P., Nayfeh, A., "Three-Dimensional Nonlinear Vibrations of Composite Beams-I. Equations of Motion", Nonlinear Dynamics, Vol. 1, 1990, pp. 477-502.

[8] Hodges, D. H., "A Mixed Variational Formulation Based on Exact Intrinsic Equations for Dynamics of Moving Beams", International Journal of Solids and Structures, Vol. 26, No. 11, 1990, pp. 1253-1273.

[9] Tang, D., Dowell, E., "Experimental and Theoretical Study on Aeroelastic Response of High-Aspect-Ratio Wings", AIAA Journal, Vol. 39, No. 8, 2001, pp. 1430-1441.

[10] Tang, D., Dowell, E., "Effects of Geometric Structural Nonlinearity on Flutter and Limit Cycle Oscillations of High-Aspect-Ratio Wings", J Fluid Structure, Vol. 19, 2004, pp. 291-306.

[11] Patil, M. J., Hodges D. H., and Cesnik, C. E. S., "Nonlinear Aeroelasticity and Flight Dynamics of High-Altitude, Long-Endurance Aircraft", Journal of Aircraft, Vol. 38, No. 1, 2001, pp. 88-94.

[12] Patil, M. J., Hodges, D. H., and Cesnik, C. E. S., "Nonlinear Aeroelastic Analysis of Complete Aircraft in Subsonic Flow", Journal of Aircraft, Vol. 37, No. 5, 2000, pp. 753-760.

[13] Patil, M. J., Hodges, D. H., "Limit-Cycle Oscillations in High-Aspect-Ratio Wings", J Fluids Structure, Vol. 15, 2001, pp. 107-132.

[14] Yuan, K. A., Friedmann, P. P., "Aeroelasticity and Structural Optimization of Composite Helicopter Rotor Blades with Swept Tips", NASA CR 4665, 1995.

[15] Yuan, K. A., Friedmann, P. P., "Structural Optimization for Vibratory Loads Reduction of Composite Helicopter Rotor Blades with Advanced Geometry Tips", Journal of the American Helicopter Society, Vol. 43, No. 3, 1998, pp. 246-256.

[16] Friedmann, P. P., Glaz, B., and Palacios, R., "A Moderate Deflection Composite Helicopter Rotor Blade Model with an Improved Cross-Sectional Analysis", International Journal of Solids and Structures, Vol. 46, 2009, pp. 2186-2200.

[17] Hodges, D. H., "Nonlinear Composite Beam Theory", AIAA, Reston, VA, 2006.

[18] Hodges, D. H., Yu, W., "A Rigorous, Engineer-Friendly Approach for Modeling Realistic, Composite Rotor Blades", Wind Energy, Vol. 10, 2007, pp. 179-193.

[19] Murugan, S., Ganguli, R., and Harursampath, D., "Effects of Structural Uncertainty on Aeroelastic Response of Composite Helicopter Rotor", 48th AIAA/ASME/ASCE/AHS/ACS Structures, Structural Dynamics and Materials Conference, Honolulu, HI, AIAA Paper 2298, 2007, pp. 1-18.

[20] Patil, M. J, Hodges, D. H., "On the Importance of Aerodynamic and Structural Geometrical Nonlinearities in Aeroelastic Behavior of High-Aspect-Ratio Wings", Journal of Fluids and Structures, Vol. 19, 2004, pp. 905-915.

[21] Librescu, L., Chiocchia, G., and Marzocca, P., "Implications of Cubic Physical/Aerodynamic Non-linearities on the Character of the Flutter Instability Boundary", International Journal of Non-linear Mechanics, Vol. 38, 2003, pp. 173-199.

[22] Ghadiri, B., Razi, M., "Limite Cycle Oscillations of Rectangular Cantilever Wings Containing Cubic Nonlinearity in an Incompressible Flow", Journal of solid and structures, Vol. 23, 2007, pp. 665-680.

[23] Hodges, D. H., "Nonlinear Equations for Dynamics of Pretwisted Beams Undergoing Small Strains and Large Rotations", NASA TP 2470, 1985.

[24] Razavi Kermanshahi, M., Lotfi Neyestanak, A. A., "Exact Vibration and Buckling Solution of Levy Type Initially Stressed Rectangular Thin Plates", Int J Advanced Design and Manufacturing Technology, Vol. 6, No. 4, 2013, pp. 65-73.

[25] Karbaschi, K., Hasanzadeh, H., "Numerical Analysis of Plate's Vibration Behavior with Non-linear Edge under Various Boundary Conditions", Int J Advanced Design and Manufacturing Technology, Vol. 1, No. 2, 2008, pp. 52-65.

[26] Kargarnovin, M. H., Karbaschi, K., and Hasanzadeh, H., "Numerical Study of Increasing Error Order in Finite Difference Method Used for Analyzing the Rectangular Isotropic Plate's Vibration Behavior", Int J Advanced Design and Manufacturing Technology, Vol. 1, No. 2, 2008, pp. 1-9.

[27] Greenberg, J. M., "Airfoil in Sinusoidal Motion in a Pulsating Stream", NACA TN 1326, 1947.

[28] Peters, D. A., Cao, W. M., "Finite State Induced Flow Models Part I: Two Dimensional Thin Airfoil", Journal of Aircraft, Vol. 32, No. 2, 1995, pp. 313-322.

[29] Patil, M. J. "Aeroelastic Tailoring of Composite Box Beams", In Proceedings of the 35th Aerospace Sciences Meeting and Exhibit, Reno, Nevada, 1997.